



Original Research Article

Advancing the understanding of silver nanoparticles removal: Comprehensive assessment-based modelling in wastewater treatment plants

Paulina Vilela^{*1}, Gabriela-Elizabeth Vilela-Govea², Johanna Vanessa Zambrano Flores³

¹ ESPOL Polytechnic University, Escuela Superior Politécnica del Litoral, ESPOL, Facultad de Ingeniería en Ciencias de la Tierra, Campus Gustavo Galindo Km. 30.5 Vía Perimetral, P.O. Box 09-01-5863, Guayaquil 090112, Ecuador

e-mail: pvilela@espol.edu.ec

² ESPOL Polytechnic University, Escuela Superior Politécnica del Litoral, ESPOL, Facultad de Ciencias Sociales y Humanísticas, Campus Gustavo Galindo Km. 30.5 Vía Perimetral, P.O. Box 09-01-5863, Guayaquil 090112, Ecuador

e-mail: gvilela@espol.edu.ec

³ cambiaMO, changing mobility, Calle del Duque de Fernán, 2, 1ª planta, Centro, Madrid 28012, Spain

e-mail: johanna.zambrano@cambiamo.net

Cite as: Vilela, P., Vilela-Govea, G. E., Zambrano Flores, J. V., Advancing the understanding of silver nanoparticles removal: Comprehensive assessment-based modelling in wastewater treatment plants, *J.sustain. dev. energy water environ. syst.*, 14(4), 1140740, 2026, DOI: <https://doi.org/10.13044/j.sdewes.d14.0740>

ABSTRACT

Silver nanoparticles discharged from wastewater treatment plants pose potential risks to aquatic environments and in long term it may cause serious human health issues, hindering life quality. Limited research has been developed, making it difficult to ensure efficient removal of silver nanoparticles in wastewater treatment plants. This study evaluates silver nanoparticles removal efficiency across different wastewater treatment plant layouts: conventional activated sludge, an anaerobic/oxic process configuration, and a 4-stage Bardenpho process system. Silver nanoparticle removal efficiency was 82% and nitrogen removal efficiency exceeded 95% under steady state conditions; however, under dynamic conditions, a significant reduction was observed in the Bardenpho and anaerobic/oxic configurations. The results also showed variability in organic matter and nitrogen removal due to reduced internal recirculation flowrates. The findings highlight the need to optimize certain configurations to ensure balanced performance across all pollutants.

KEYWORDS

Benchmark simulation, emerging contaminants, silver nanoparticle removal, wastewater treatment modelling, wastewater treatment plants

INTRODUCTION

The accelerated pace of industrial development, while addressing growing societal demands, has also intensified environmental degradation, influencing the discharge of untreated wastewater containing synthetic dyes, heavy metals, and other hazardous substances [1]. Silver nanoparticles (AgNPs) have become key ingredients in a wide range of consumer products [2], including medical devices, textiles, and electronics, owing to their unique antimicrobial properties and versatile applications [3]. They have physicochemical traits that combined with their versatility, allow their incorporation into a wide array of consumer

^{*} Corresponding author

products [4]. Their efficacy in inhibiting microbial growth and even viral activity positions them as promising alternatives to conventional antibiotics [5], and recently it has been studied as an added nanomaterial to enhance wastewater treatment [6]. The biological activity and functional performance of AgNPs are governed by multiple factors, such as particle size and shape, composition, surface chemistry, capping agents, dissolution rate, agglomeration state, and ion release behaviour in aqueous environments [3]. This dual nature, both therapeutic and potentially hazardous, turns them into emerging contaminants that need the development of better comprehensive toxicity assessments [7]. However, their increasing prevalence has raised significant concerns about the potential risks they pose to human health and the environment [8].

AgNPs often bypass conventional wastewater treatment plants (WWTPs) [9], potentially disrupting microbial communities essential for maintaining wastewater treatment efficiency [10]. This poses a threat to the stability and efficiency of wastewater treatment plants [11], particularly through the disruption of microbial communities, vital for pollutant degradation [12]. Although AgNPs are increasingly employed in water remediation strategies [6], their persistence and interactions within treatment systems remain poorly understood [13]. For instance, studies show that in the sludge from WWTPs, AgNPs have portrayed negative effects, causing biotic stress and problems with settling performance. Given that the bacteria in WWTPs coordinate their behaviour for suspension and diffusion growth, it is altered by the AgNP concentration in the deterioration of the sludge floc structure [14]. Similarly, AgNPs have shown that they can be mostly removed through the sludge of WWTPs, where at least 90% of the nanoparticles contents is accumulated [15]. However, the behaviour of AgNPs in the main treatment line of WWTPs remains insufficiently understood, and few studies have been conducted to date. The persistence of the remaining AgNP in wastewater systems highlights the urgent need for a deeper understanding of their environmental behaviour and effects in WWTPs.

Over the past decades, mathematical modelling has been utilized for understanding and designing WWTPs. Activated sludge models (ASMs), developed by the International Water Association (IWA), have been widely adopted in literature to simulate biological nutrient removal processes [16]. These models are able to represent the complex microbial interactions, physicochemical processes encountered in WWTPs, allowing to analyse system behaviour effectively [17]. Consequently, process modelling to study removal treatment efficiency, WWTP design, and fate of contaminants, the Benchmark simulation frameworks, such as the Benchmark Simulation Model No. 1 (BSM1), have further been implemented [18]. Several studies have applied ASM and BSM modelling to analyse treatment performance and evaluate control strategies in WWTPs. For instance, ASM was used to reproduce the performance of industrial and municipal WWTPs and to optimize operational conditions [19], and BSM1 was used to evaluate advanced control strategies under dynamic influent conditions [20]. The integration of emerging contaminants represents a relevant study direction, to assess contaminant fate and potential impacts without the limitations of full-scale studies.

Regarding AgNP removal in WWTPs, studies have shown that nitrogen removal is influenced by the nanoparticles action [21], indicating that AgNPs affect the biological treatment efficiency [22]. In addition, most AgNPs adsorb onto sludge particles, which may further influence microbial performance and system stability [23]. More studies suggest that while AgNPs can be partially removed through biological treatment processes such as activated sludge [5], their removal efficiency depends on several parameters, including particle properties, contact time, solution chemistry, and the presence of extracellular polymeric substances (EPS) [24]. Previous research has also highlighted this importance as well and took representative mechanisms of AgNP (adsorption-desorption, inhibition, dissolution, and chemical precipitation) [25], and have applied them into an activated sludge model (ASM-AgNP) [26]. Different AgNPs sizes and influent concentrations were considered, proving good removal efficiency of all the parameters like nitrogen, chemical oxygen demand, and AgNPs

[26]. Considering that particles characteristics and fate mechanisms might have direct relation to the treatment conditions of WWTPs, the present study investigates the removal efficiency in plants utilizing the ASM-AgNP model for different WWTPs to expand the understanding of AgNPs removal.

Despite numerous investigations presenting the effects of AgNPs on microbial communities and biological treatment, limited research has been conducted on their influence on varied WWTP configurations, considering their physical conditions and treatment lines, with their most known fate mechanisms, such as adsorption, dissolution and inhibition. Given these challenges, it is essential to gain insight into how different wastewater treatment plant configurations manage AgNP concentrations and how it influences biological treatment performance. This study aims to (i) assess the removal efficiency of AgNPs and nitrogen species using the ASM-AgNP modelling; (ii) compare the performance in three wastewater treatment plant configurations under steady state and dynamic conditions: Benchmark Simulation Model No. 1 (BSM1), Bardenpho process, and Anaerobic/Oxic (A/O) process; and (iii) evaluate the influence of system configuration on treatment efficiency and effluent quality. By employing dynamic modelling, this research seeks to evaluate treatment strategies conditions and contribute to a better understanding of the environmental behaviour of AgNPs in wastewater treatment infrastructure. The structure of the study follows an introduction where the major fundamentals and objectives are presented, a methodology with a description of the models and the equations utilized, results and discussion with a description of the evaluation of results, and finally the conclusions.

MATERIALS AND METHODS

This study adopts a schematic research framework for modelling a wastewater treatment system, considering biological treatment using the activated sludge process. The modelling was performed under steady state and dynamic conditions. The activated sludge model with silver nanoparticles (ASM-AgNP) from Vilela *et al.* [26], is used as a base model that has been already validated for wastewater treatment plants (WWTPs) within the BSM1 and the activated sludge model No. 1 (ASM1). The effluent quality of the results is evaluated with the parameters: chemical oxygen demand (COD), biological oxygen demand (BOD), nitrite (NO_2^-), nitrate (NO_3^-), ammonia nitrogen ($\text{NH}_4^+\text{-N}$), and total nitrogen (TN). The following sections explain the further steps taken within the development of this study and the dynamic simulations.

Evaluation framework

A framework of the study is presented in Figure 1. It illustrates the methodology for analyzing the behaviour of AgNPs in WWTPs through the simulations of the ASM-AgNP within the BSM1 (BSM1-AgNP), bardenpho 4-stage model (Bardenpho-AgNP), and the anoxic/oxic model (A/O-AgNP). Furthermore, the removal efficiency of AgNPs is evaluated in the WWTP layouts and compared to the baseline BSM1 without AgNPs. The ASM-AgNP model was developed by Vilela *et al.* [26], based on the conditions established by the International Water Association (IWA) [18]. The variables and process rates that are utilized in this model are presented in Figure 2.

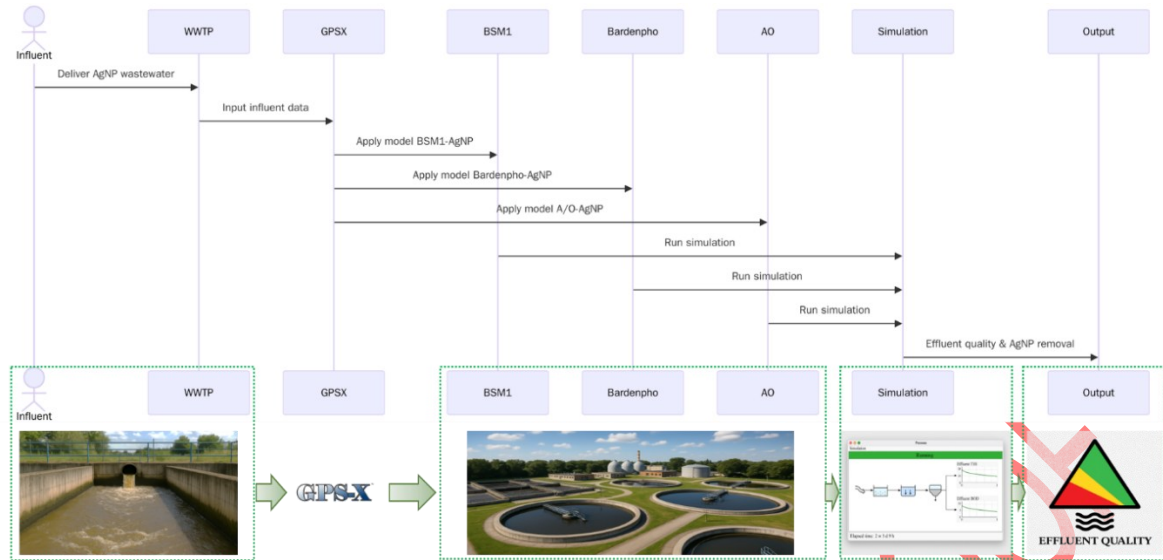


Figure 1. Sequence-wise framework of the study.

No.	Process	Variables																		
		1	2	3	4	5	6	7	8	9	10	11	12	13	14	15	16	17	18	
		S_1	S_2	X_1	X_2	X_{NH}	X_{NA}	X_P	S_{O_2}	S_{NO_3}	S_{NH_4}	S_{NO_2}	X_{NO}	S_{ALK}	S_{Ag}	S_{Ag}	X_{Ag}	$NaOH$	X_{pAg}	
1	Acrobic growth of heterotrophs		-1.4925			1			-0.492537											
2	Anoxic growth of heterotrophs		-1.4925			1				0.17238										
3	Acrobic growth of autotrophs						1		-18.04761	4.16666	4.252667									
4	Decay of heterotrophs				0.92	-1		0.08					0.0812							
5	Decay of autotrophs				0.92		-1	0.08					0.0812							
6	Ammonification of soluble organic nitrogen										1	-1		0.071429						
7	Hydrolysis of entrapped organics		1		-1															
8	Hydrolysis of entrapped organic nitrogen											1	-1							
9	Adsorption of AgNP to biomass															-1		1		
10	Desorption of adsorbed AgNP															1		-1		
11	Dissolution of AgNP to Ag ion															-1		1		
12	Chemical precipitation of Ag ion																	-1		1

Figure 2. ASM-AgNP model's Petersen matrix. Adapted from Vilela et al. [26].

Suitable coefficients and process rates for the removal mechanisms were determined and calculated in [26], where the authors performed a system analysis and validated the model's response to varying nanomaterial influent concentrations. The model also includes chemical precipitation to improve the removal efficiency of AgNPs. In this study, hydroxide precipitation was applied to enable comparisons with previous work. Sodium hydroxide (NaOH) is utilized to facilitate easy solid-liquid separation [27].

Model development

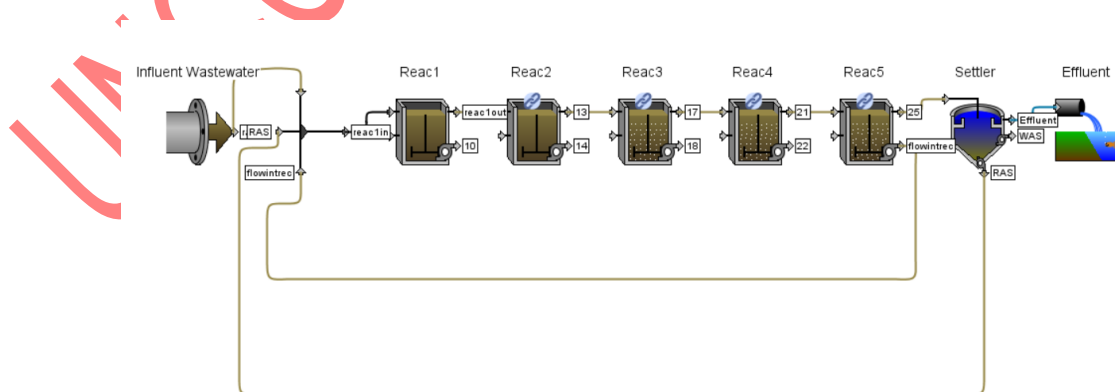
This study used GPS-X version 8.0.1 software for technical and qualitative analyses of the three WWTP configurations for AgNP: BSM1 with AgNP (BSM1-AgNP), Bardenpho 4-stage model with AgNP (Bardenpho-AgNP), and AO model with AgNP (A/O-AgNP), and the baseline model BSM1 without AgNPs. The model development follows the tool of model developer from the software. The whole stoichiometry and kinetics of the ASM-AgNP model were implemented and then generated with the model developer tool.

Furthermore, the operational parameters and characteristics summarized in Table 1 followed the standard BSM1 framework to ensure comparability. The conditions for influent characteristics, flowrate, sludge retention time, aeration, and sludge were maintained. The primary differences among the studied configurations are the physical configuration and the internal recycle flowrate, with the BSM1 as a baseline. These variations in hydraulic and process design are critical factors influencing nutrient removal and organic matter degradation.

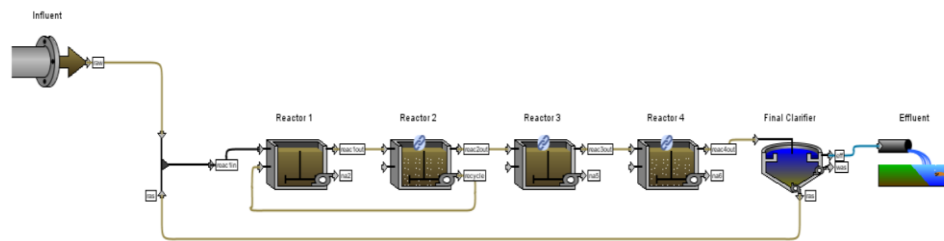
Table 1. Operational parameters and characteristics of the WWTP model configurations.

Parameter	Conditions based on BSM1	BSM1-AgNP	Bardenpho-AgNP	A/O-AgNP
Influent flowrate (Q)	18,446 m ³ /d			
Sludge retention time (SRT)	10 days			
Dissolved oxygen (DO)	2.0 mg/L (aerobic zones, controlled in final reactor)	2.0 mg/L (aerobic zones)		
Temperature	Standard conditions: ~20 °C typical	20 °C		
Return activated sludge (RAS)	18,446 m ³ /d			
Waste activated sludge (WAS)	385 m ³ /d			
Internal recycle (range)	0–5Q (typical 3Q)	3Q	3Q	–
Number of reactors	5-stage (2 anoxic + 3 aerobic)	5-stage (2 anoxic + 3 aerobic)	4-stage Bardenpho (2 anoxic + 2 aerobic)	2-stage A/O (1 anoxic + 1 aerobic)

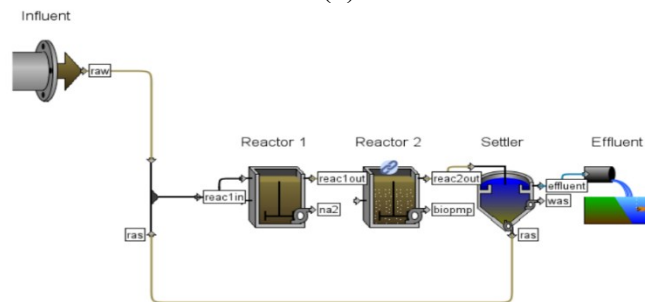
The different configurations developed in GPS-X are presented in Figure 3. The key dimensions of the suggested approach are as follows: First, the ASM1-AgNP model is configured in GPS-X; second, the BSM1-AgNP, Bardenpho-AgNP and A/O-AgNP models are developed; third, the influent/sludge characteristics and operating parameters of the biological model are calibrated to the base model; fourth, the validity of the steady and dynamic simulations are evaluated on every model. The dynamic simulations were performed following the standard BSM1 dynamic conditions presented by Alex et al. [18]. The simulation time is 14 days, and to analyse the results the end of the simulation period is taken. The initial phase of the simulation describes the system stabilization; thus, the performance evaluation is focused on the end of the simulation period.



(a)



(b)



(c)

Figure 3. Wastewater treatment plant configurations evaluated in this study: (a) BSM1 with AgNP (BSM1-AgNP); (b) Bardenpho 4-stage model with AgNP (Bardenpho-AgNP); and (c) AO model with AgNP (A/O-AgNP). The diagrams were taken from GPS-X.

Furthermore, the influent concentrations were primarily adopted from the BSM1 report [18], and the AgNP concentrations utilized in the WWTP models were of 14.92 mg/L for AgNPs and 72.24 mg/L for Ag ion, adopted from the study of Cervantes-Avilés et al. [28]. The same value of 14.92 mg/L was used in all configurations, helping to perform a direct comparison between them for the calculated removal efficiencies. The influent AgNP concentration represents a worst-case scenario, with high nanomaterial levels used to evaluate system robustness rather than typical environmental conditions. Although it is known that typical environmental concentrations of AgNPs are generally reported at lower levels, higher concentrations were adopted to evaluate robustness and sensitivity of the treatment configurations. This allows an assessment of system behaviour, potential inhibition effects and removal performance. Given the scarcity of research and difficulty carrying out large scale experiments, this data has been fully adopted from published works. Hence, to partially overcome this limitation, comparisons with BSM1 without AgNPs, the baseline model, are made to analyse the validity of the results from the models. The stoichiometric processes that the model implemented for AgNP, adapted from [21] and [22], come from the mass balances presented in the following equations [eq. (1), eq. (2), eq. (3) and eq. (4)]:

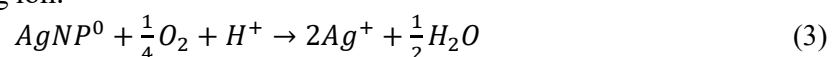
Adsorption of AgNP to biomass:



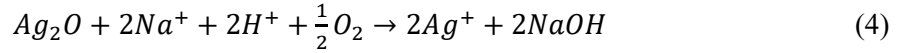
Desorption of adsorbed AgNP:



Dissolution of AgNP to Ag ion:



Chemical precipitation of Ag ion:



where S_{ag} is the AgNP in mg/L, $X_{BH} + X_{BA}$ (mg COD/L) represent the biomass in mg COD/L, X_{ag} is the adsorbed AgNP in mg/L, $AgNP^0$ is the silver concentration in mg/L, Ag^+ is the silver ion concentration in mg/L, O_2 is oxygen concentration, H^+ is hydrogen concentration, H_2O is water concentration, Na^+ is sodium concentration, and $NaOH$ is the sodium hydroxide concentration in mg/L.

Performance assessment in wastewater treatment plant configurations

The effluent quality assessment is performed following the BSM1 report firstly, given that the ASM-AgNP was derived from it. The conditions for the evaluation were: total nitrogen (TN) should be less than 18 mg/L, total chemical oxygen demand (COD_t) less than 100 mg/L, nitrogen ammonia less than 4 mg/L, BOD_t less than 10 mg/L [18]. In addition, the effluent quality index (EQI) has been estimated to measure the quality of the removal resulting from each WWTP configuration. Equation (5) shows the EQI calculation, and the variables considered for this analysis [18]:

$$EQI = \frac{1}{T \cdot 1000} \int_{7d}^{14d} \left(\frac{b_{SS} * SS_{eff}(t) + b_{COD} * COD_{eff}(t) + b_{Nkj} * S_{Nkj,eff}(t) + b_{NO} * S_{NO,eff}(t) + b_{BOD5} * BOD_{eff}(t)}{Q_{eff}(t)} \right) dt \quad (5)$$

where the b_i are the weighting factors assigned for each variable and the concentrations of the variables are taken in g/m³. All the b_i values have been adopted from the BSM1 report, being b_{SS} 2 g contaminant*g, b_{COD} 1 g contaminant*g, b_{Nkj} 30 g contaminant*g, b_{NO} 10 g contaminant*g, b_{BOD5} 2 g contaminant*g [18]. Furthermore, each variable [eq. (6), eq. (7), eq. (8), and (9)] represents the sum of the different variables in the model at the effluent:

$$S_{Nkj,eff} = S_{NH,eff} + S_{ND,eff} + X_{ND,eff} + I_{XB}(X_{BH,eff} + X_{BA,eff}) + I_{XP}(X_{P,eff} + X_{I,eff}) \quad (6)$$

$$SS_{eff} = 0.75(X_{S,eff} + X_{I,eff} + X_{BH,eff} + X_{BA,e} + X_{P,eff}) \quad (7)$$

$$BOD_{5,eff} = 0.25 \left(S_{S,eff} + X_{S,eff} + (1 - f_p) \cdot (X_{BH,eff} + X_{BA,eff}) \right) \quad (8)$$

$$COD_{eff} = S_{S,eff} + S_{I,eff} + X_{S,eff} + X_{I,eff} + X_{BH,eff} + X_{BA,eff} + X_{P,eff} \quad (9)$$

where all the variables have the subscript eff, representing the values in the effluent concentration. For these, $S_{Nkj,eff}$ is the Kjeldahl nitrogen in the effluent concentration, which is the sum of the soluble and particulate nitrogen in the model; SS_{eff} is the suspended solids of the effluent concentration; $BOD_{5,eff}$ is the BOD concentration at the effluent; and COD_{eff} is the effluent concentration of COD.

Furthermore, removal efficiencies were calculated following standard procedures. For steady state conditions, constant influent concentrations from the BSM1 were used. For dynamic state conditions, removal efficiencies were calculated based on the average influent concentrations over the evaluation period. For AgNPs, removal efficiency is defined based on total AgNP concentration, including both soluble and particulate fractions considered in the model. Two removal approaches are considered, first, the overall removal, which accounts for total mass removal and sedimentation; second, the removal calculated with the effluent of the AgNP concentration, estimated with the influent and effluent in the liquid phase. The standard expression used to estimate removal efficiency is presented in eq. (10) **Error! Reference source not found.:**

$$RemEff(\%) = \left(\frac{C_{in} - C_{eff}}{C_{in}} \right) \times 100 \quad (10)$$

where C_{in} and C_{eff} represent the influent and effluent concentrations (mg/L), respectively.

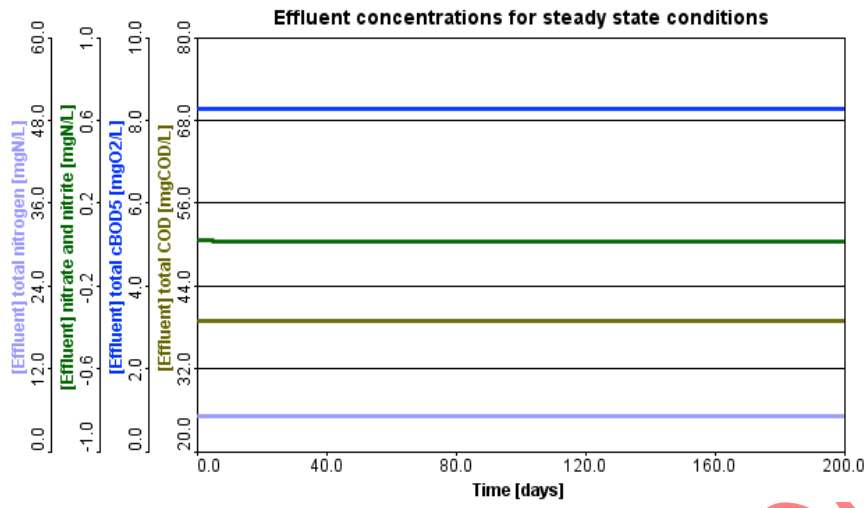
RESULTS AND DISCUSSION

This section describes all the results and discussions obtained in this study. The results are presented by categories, divided into sub-sections, as follows:

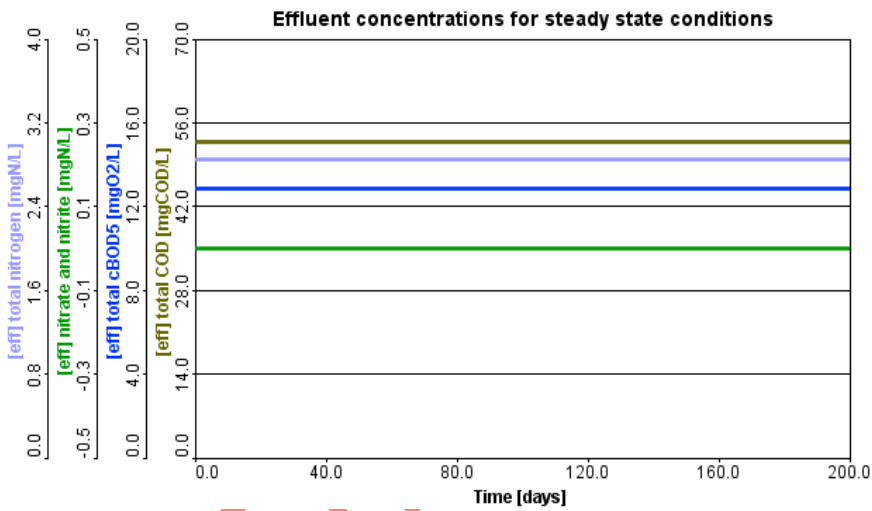
Removal in wastewater treatment plants for steady state

Figure 4 shows the results obtained at the effluent of the models' simulations with base influent conditions, which were taken from the BSM1, for steady state conditions. The concentrations of total nitrogen (TN), nitrate/nitrite nitrogen (NO_3/NO_2), total biochemical oxygen demand (BOD_t), and total chemical oxygen demand (COD_t) are shown. Figure 4a corresponds to a TN value of 4.57 mg/L, NO_3/NO_2 value of 0.034 mg/L, BOD_t value of 7.53 mg/L, and COD_t value of 46.11 mg/L, from the BSM1-AgNP model. These values fall within the values set from results for the BSM1. The total COD shows a slightly higher value than the one from the base BSM1, however, this might be related to the difference in estimation adhered to the simulation software GPS-X [29]. It is known that the software can present some difference in decimals as the calculations are shortened in some instances [30]. It should be noted that the values presented in the figures are approximate graphical representations, while the numerical values reported in the text correspond to the exact simulation outputs obtained from GPS-X.

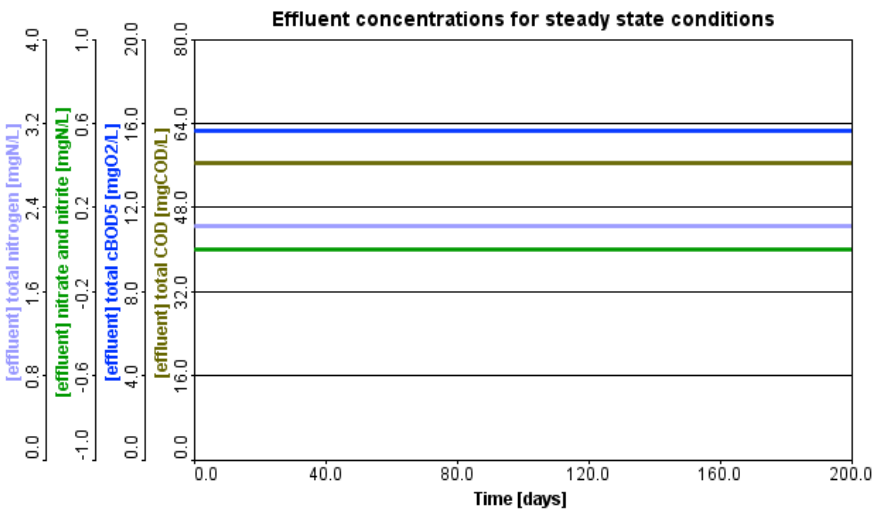
Compared to the baseline BSM1 without AgNPs results in Figure 4d, the model performed with similar results, giving final effluent concentrations of around the values with a difference of some decimals, for instance, COD_t was 39.1 mg/L and TN was 5.33 mg/L in the BSM1. The major highlight is that the concentration of TN in the BSM1-AgNP is a little lower than in the BSM1, representing similar removal for both. Moreover, for AgNPs a high removal was observed, obtaining an average effluent concentration of 2.7 mg/L for all the WWTP configurations, as shown in Figure 5, and it did not interfere with the removal of the rest of the components considered in this analysis, such as TN, COD, and BOD.



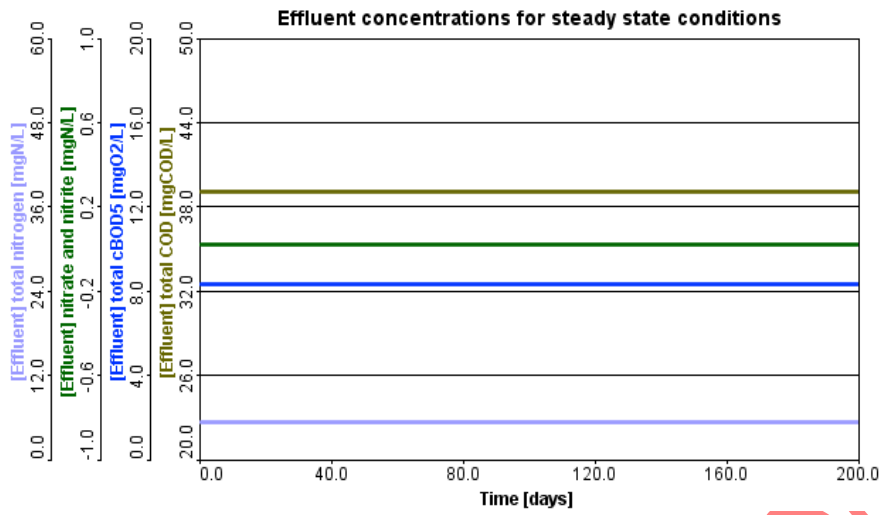
(a)



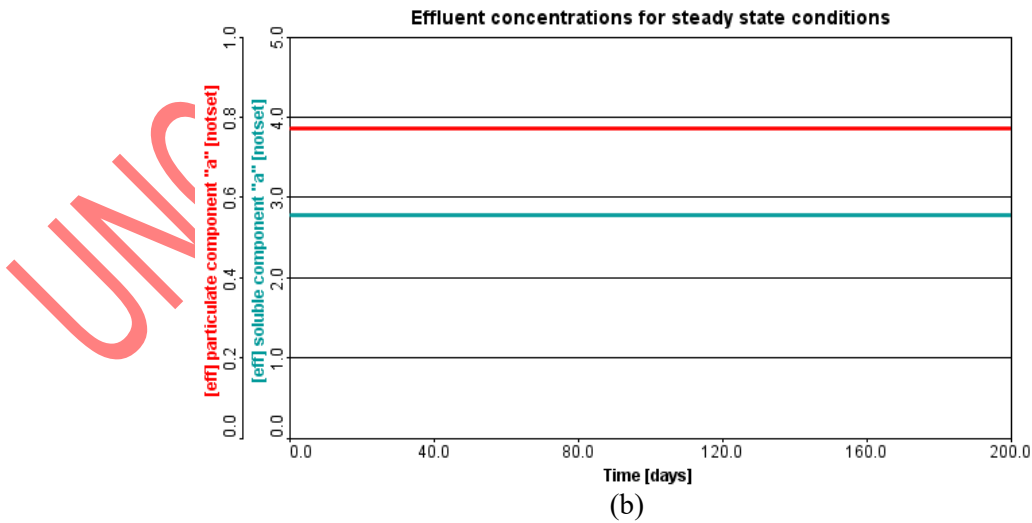
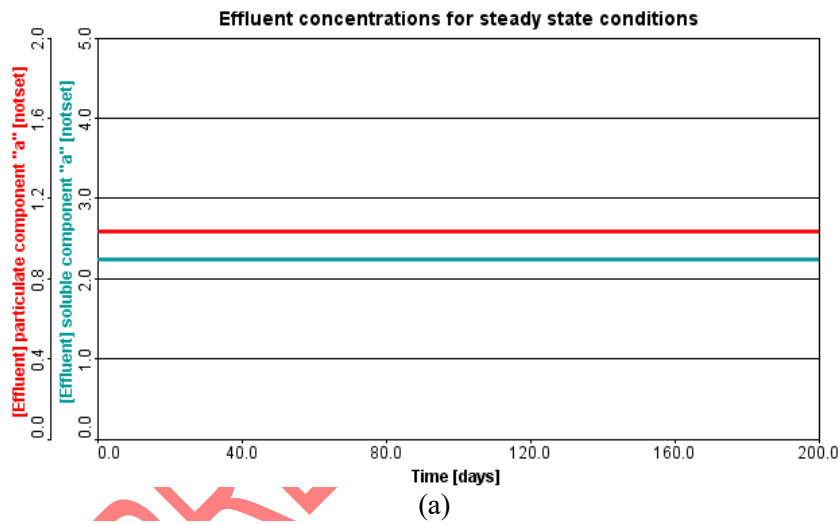
(b)



(c)



(d)
 Figure 4. Effluent concentrations for steady state conditions in the: (a) BSM1-AgNP model, (b) Bardenpho-AgNP, (c) A/O-AgNP, and (d) BSM1 without AgNPs as the baseline configuration.



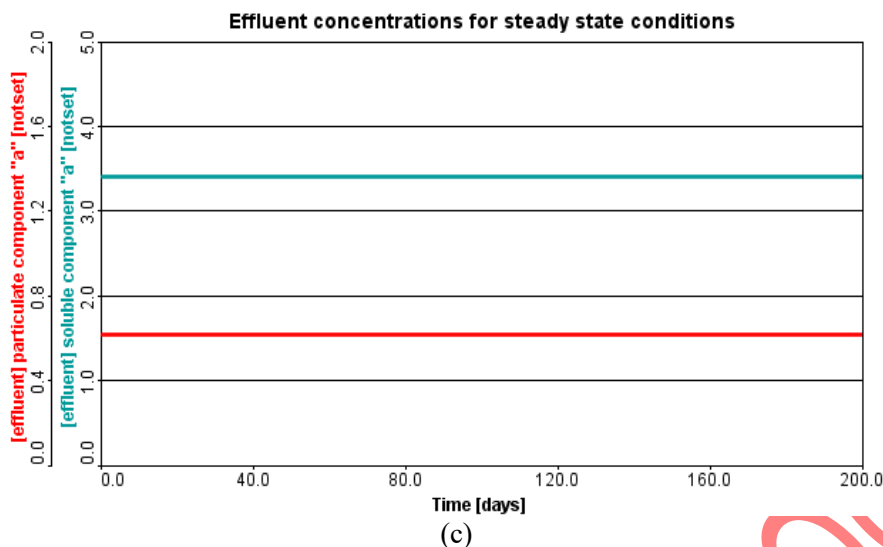


Figure 5. Effluent AgNP concentrations for steady state conditions, where soluble component a represents AgNP and particulate component a represents particulate AgNP in the: (a) BSM1-AgNP model, (b) Bardenpho-AgNP, and (c) A/O-AgNP.

Following with the analysis, Figure 4b corresponds to a TN value of 2.22 mg/L, NO₃/NO₂ reached a zero value, BOD_t value of 12.85 mg/L, and COD_t value of 52.79 mg/L, from the Bardenpho-AgNP model. Finally, Figure 4c corresponds to a TN value of 2.85 mg/L, NO₃/NO₂ reached a zero value, BOD_t value of 15.65 mg/L, and COD_t value of 56.56 mg/L, from the A/O-AgNP model. For these two model configurations, the results show higher concentration of COD, which is related to the physical conditions of a smaller number of reactors and lower or absent internal recycle flowrates in them. This provides an insight into the influence of the recycle flowrate in wastewater treatment plants, to provide better conditions for good COD removal efficiency. Moreover, the BSM1 model without the AgNP concentration represented final values of COD_t 39.1 mg/L and TN 5.33 mg/L as presented in Figure 4d, which, when compared to the Bardenpho-AgNP model, indicates that the TN removal was higher and that the COD removal was lower. Similarly, comparing the Bardenpho-AgNP model, the TN was lower and the COD_t was a little higher but in the same range, both showing a good removal in this configuration. Meanwhile, for the A/O-AgNP model, the TN had equally a low value and a small increase of COD_t compared to the results from BSM1. Hence, both configurations show good removal results. In general, both configurations showed similar behaviour for steady state conditions.

Table 2 summarizes the steady state performance of the WWTP configurations, integrating effluent concentrations, removal efficiencies, and EQI values. It is noted that removal efficiencies were calculated based on influent and effluent concentrations, in agreement with the values presented in the figures and tables. For AgNPs, the reported percentages correspond to effluent-based removal, aligned with the observed concentration reduction, considering combined soluble and particulate AgNPs in the model. The results indicate that all configurations achieved high treatment efficiencies, particularly for BOD removal, exceeding 90% especially in the BSM1-AgNP configuration. Nitrogen removal efficiencies were also consistently high, in contrast, COD removal showed lower efficiencies in Bardenpho-AgNP and A/O-AgNP configurations. The EQI results further confirmed that the BSM1-AgNP configuration provides the best overall effluent quality. Higher EQI values represent a relation to increased residual organic matter in the effluent.

Table 2. Overall results for steady state conditions corresponding to effluent based removal.

Configuration	TN (mg/L)	TN removal (%)	COD (mg/L)	COD removal (%)	BOD (mg/L)	BOD removal (%)	AgNP (mg/L)	AgNP removal (%)	EQI (kg·units/d)
---------------	-----------	----------------	------------	-----------------	------------	-----------------	-------------	------------------	------------------

BSM1-AgNP	4.57	84.8	46.11	84.6	7.53	96.2	~2.7	>81	5455
Bardenpho-AgNP	2.22	92.6	52.79	82.4	12.85	93.6	~2.7	>81	11310
A/O-AgNP	2.85	90.5	56.56	81.1	15.65	92.2	~2.7	>81	13700

Overall, as shown in Figure 6, the steady state removal efficiencies, estimated using standard BSM1 as a baseline. BOD removal exceeded 90% in all the configurations, reaching its highest value in the BSM1-AgNP configuration, with approximately 96%. This removal may indicate strong biodegradation under stable conditions. Nitrogen removal efficiencies were 85% in BSM1-AgNP and over 92% in the Bardenpho-AgNP configuration, suggesting enhanced denitrification processes. Furthermore, COD removal was slightly lower, 81% and 85%, in the Bardenpho and A/O configurations, respectively. This result might present a relation to the low internal recirculation flowrate and the number of reactors that have each configuration. The steady state results show that all configurations provide robust treatment performance, especially the BSM1-AgNP, with a more stable removal efficiency for all the parameters.

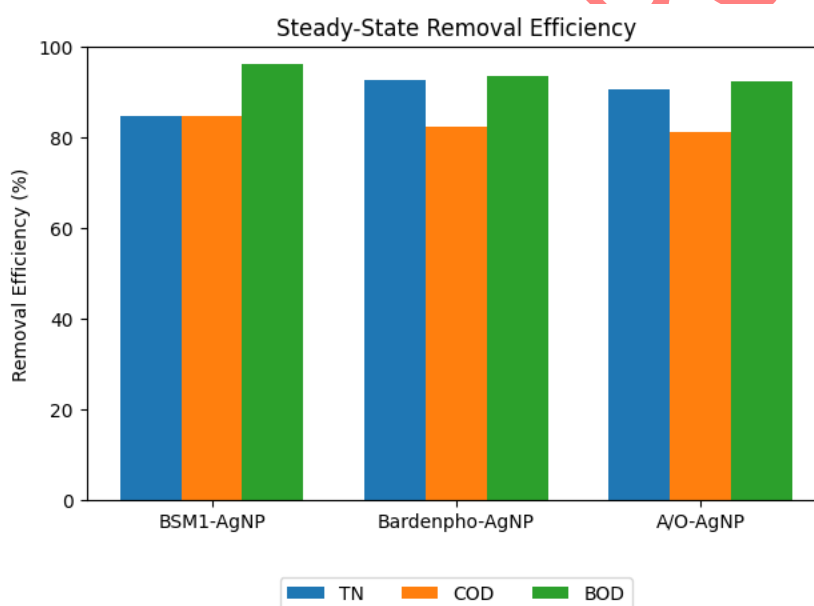
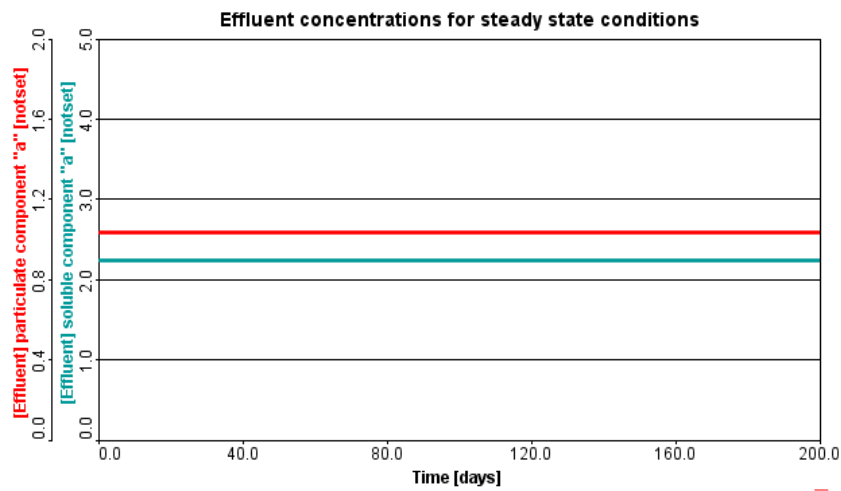


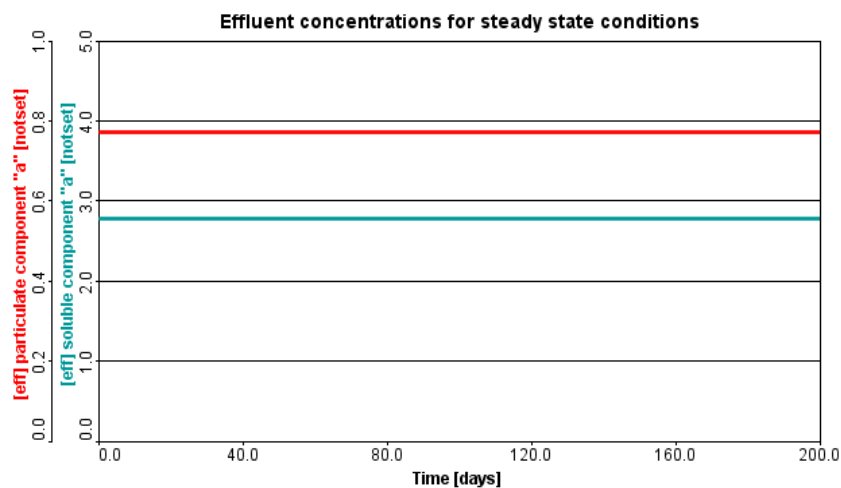
Figure 6. Removal efficiencies in steady state for the BSM1-AgNP, Bardenpho-AgNP, and A/O-AgNP model.

Removal in wastewater treatment plants for dynamic state

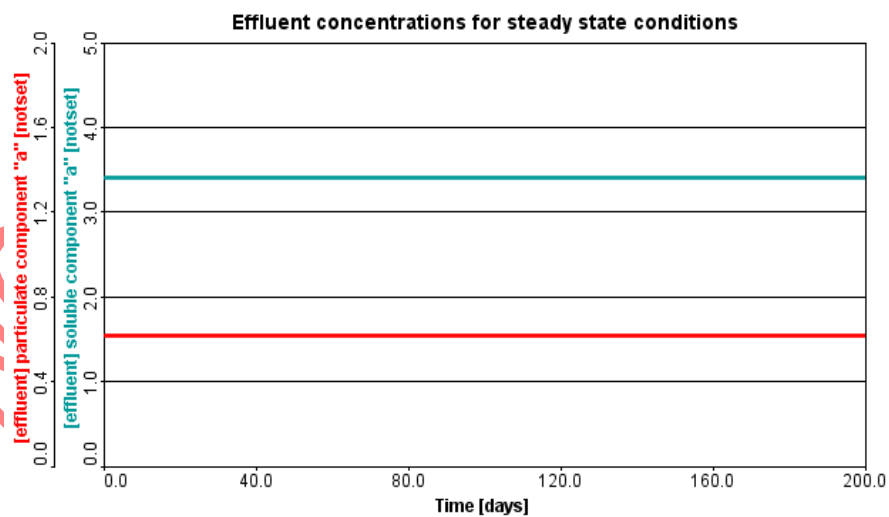
The results for AgNP concentrations in dynamic conditions (AgNP and particulate AgNP) are shown in Figure 7, portraying similar behaviour and average value of 2.2 mg/L.



(a)



(b)

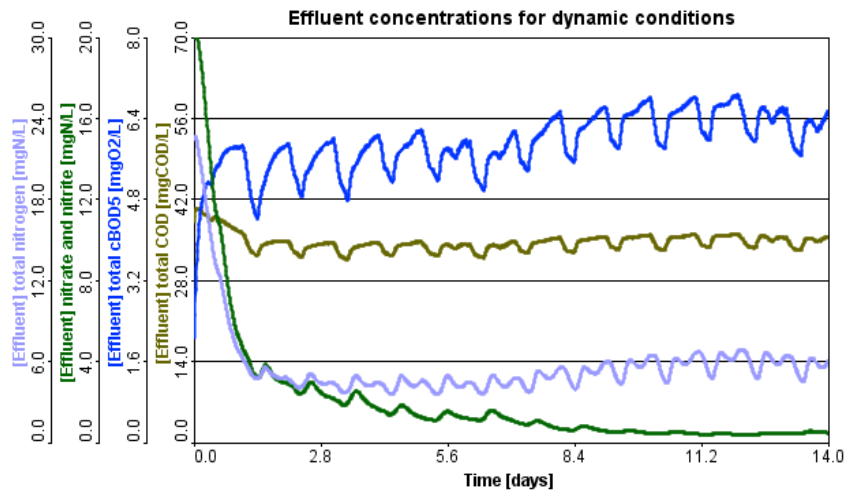


(c)

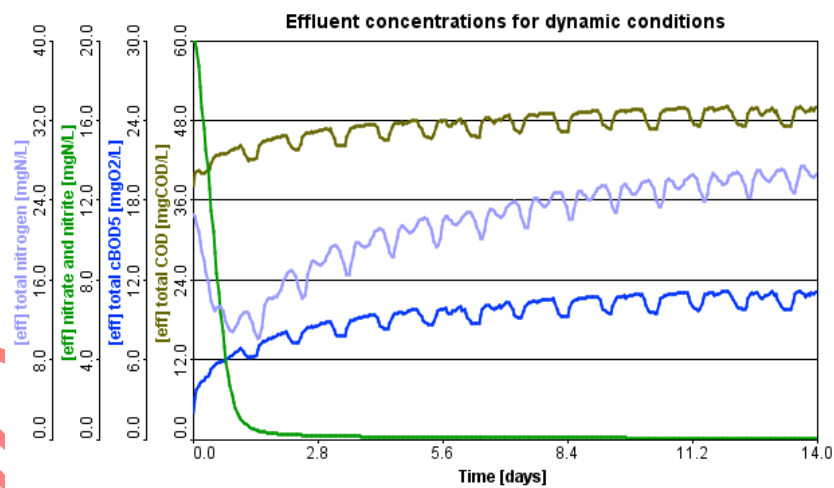
Figure 7. Effluent AgNP concentrations for dynamic conditions, where soluble component a represents AgNP and particulate component a represents particulate AgNP in the: (a) BSM1-AgNP model, (b) Bardenpho-AgNP, and (c) A/O-AgNP.

Moreover, Figure 8 shows the results for the dynamic conditions of the models' simulations. Figure 8a corresponds to a TN value at 14 days of 11.34 mg/L, NO₃/NO₂ value at 14 days of 0.68 mg/L, BOD_t value at 14 days of 6.03 mg/L, and COD_t value at 14 days of 43.04 mg/L, from the BSM1-AgNP. The values of TN and BOD are slightly different, being lower than and higher than

the described in the BSM1 report, respectively. This might be related to the stoichiometric and physical conditions of the model. Furthermore, Figure 8b corresponds to a TN value at 14 days of 26.68 mg/L, NO₃/NO₂ value at 14 days of 0.053 mg/L, BOD_t value at 14 days of 11.18 mg/L, and COD_t value at 14 days of 49.83 mg/L, from the Bardenpho-AgNP. The values of TN, BOD, and COD are higher than the ones described in the BSM1 report and the BSM1-AgNP. However, this did not interfere in the performance simulation of the model. Furthermore, the BSM1 model without the AgNPs final effluent concentration values, for dynamic conditions, of COD_t 35.07 mg/L and TN 5.81 mg/L, as presented in Figure 8d, which compared to the BSM1-AgNP model, represents a lower value, indicating that the removal of nitrogen and COD was not as good in the BSM1-AgNP. Compared to the Bardenpho-AgNP, the results are consistent with previous observations, TN and COD were less removed with a small difference.



(a)



(b)

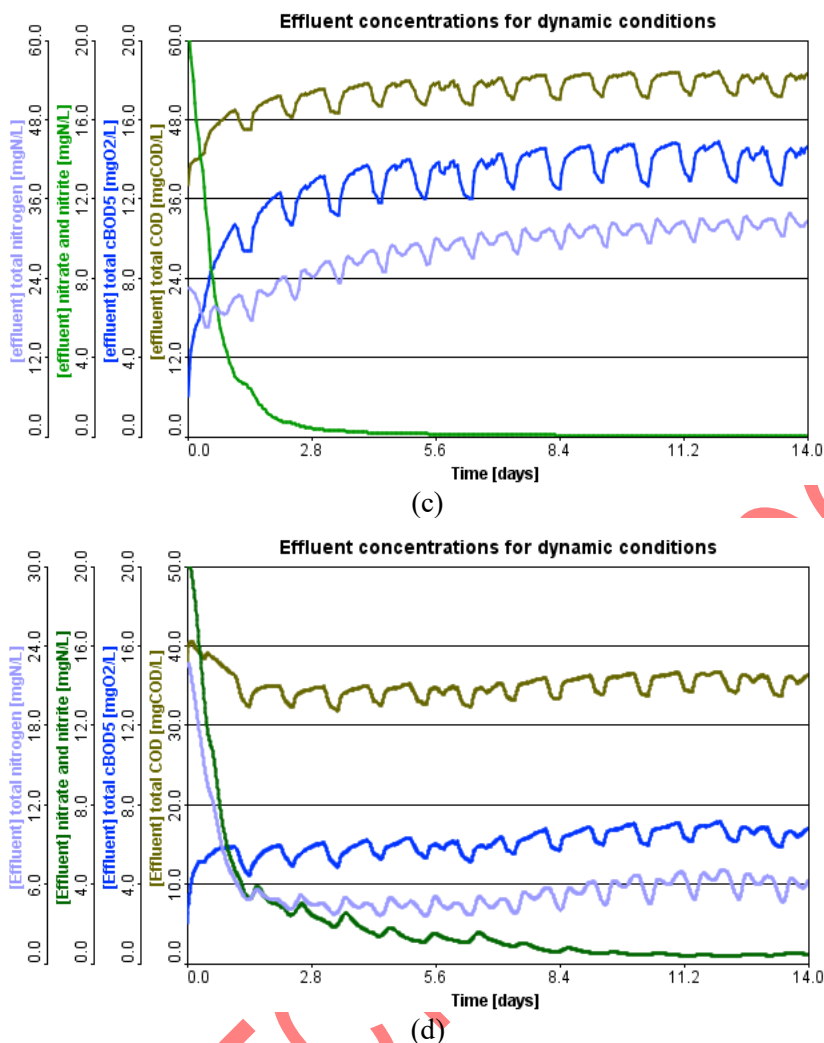


Figure 8. Effluent concentrations for dynamic conditions in the: (a) BSM1-AgNP model, (b) Bardenpho-AgNP, (c) A/O-AgNP, and (d) BSM1 without AgNPs as the baseline configuration.

Finally, Figure 8c corresponds to a TN value at 14 days of 32.2 mg/L, NO₃/NO₂ value at 14 days of 0.022 mg/L, BOD_t value at 14 days of 14.69 mg/L, and COD_t value at 14 days of 54.74 mg/L, from the A/O-AgNP model. Compared to the BSM1-AgNP, the results show an increase in effluent concentration for all the components. BSM1 describes dynamic results of average TN 15.57 mg/L, BOD_t 2.77 mg/L, COD_t 48.30 mg/L [18], compared to these values, the results obtained with BSM1-AgNP model fell around, accounting again for the difference of decimals that the software has. The Bardenpho-AgNP model results showed higher content of TN in the effluent, as well a more considerable increase in BOD_t, but with a value around the same range for COD_t. Comparing to the BSM1 model without the AgNPs final concentration values (COD_t 35.07 mg/L and TN 5.81 mg/L), as shown in Figure 8d, the A/O-AgNP presented less removal for both variables.

For the A/O-AgNP model, the TN was approximately double than that reported in BSM1, as well as for the BOD_t increasing by seven times, but with a COD_t around the range. The last two configurations thereby show that the conditions for treatment require adaptation of physical conditions and probable enhancement of stoichiometric factors. In addition, in comparison with the AgNP concentrations of Figure 7, a similar behaviour was observed, with high removal of soluble and particulate AgNP in water. Compared to previous studies, the Bardenpho and A/O configuration types, have been commonly used for large WWTPs with good performance on removal, retaining carbon, nitrogen and phosphorus from wastewater [31]. In general, when analysing the removal portrayed by the three configurations, they achieved satisfactory results for AgNP removal, and an increase in TN and COD_t was noticed for two of the configurations, which

comparing to the literature, can be related to the inhibition that AgNPs have on nitrogen removal in the activated sludge process [28].

Table 3 presents the dynamic performance of the WWTP configurations at the last 14 days of simulation. Thus, a significant reduction in nitrogen removal efficiency was observed, particularly in the Bardenpho-AgNP and A/O-AgNP configurations. This behaviour shows that these configurations might require improved operational control. In contrast, BOD removal remains consistently high while COD removal shows moderate stability. Furthermore, the EQI is only calculated for steady state conditions, as stated for BSM1, given that under dynamic conditions the analysis is over a simulation period and varies in this period. A dynamic EQI was considered not required for the scope of this study.

Table 3. Overall results for dynamic state conditions corresponding to effluent based removal.

Configuration	TN (mg/L)	TN removal (%)	COD (mg/L)	COD removal (%)	BOD (mg/L)	BOD removal (%)	AgNP removal (%)
BSM1-AgNP	11.34	62.2	43.04	85.7	6.03	97	>81
Bardenpho-AgNP	26.68	11.1	49.83	83.4	11.18	94.4	>81
A/O-AgNP	32.2	~0	54.74	81.8	14.69	92.7	>81

In treatment performance, a reduction in removal efficiency was noted, compared to the previous stage and the BSM1 as a baseline. Figure 9 presents the BSM1-AgNP configuration with a TN removal efficiency of approximately 62%, whereas the Bardenpho-AgNP and A/O-AgNP configurations showed a nearly 11% removal efficiency. These results might represent a sensitivity to the loading conditions, which sets a target to implement control strategies or operational adjustments to make improvements in the system. In contrast, BOD removal was consistent with a value higher than 92% in all configurations, which is related to organic matter degradation. COD removal efficiencies remained between 81 to 86%, indicating a lower effect on carbon removal processes than nitrogen. Thus, dynamic operation reveals limitations for nitrogen removal, particularly in the configurations with a reduced internal recirculation.

Overall, the results indicate that while all configurations perform well under steady state conditions, their behaviour under dynamic conditions differs. The BSM1 configuration shows greater robustness, which can be related to its higher internal recirculation and the number of reactors, given that this system is designed to work for nitrification-denitrification processes. On the other hand, the Bardenpho and A/O configurations showed greater sensitivity under dynamic conditions, which is likely related to the reduced internal recycle and lower number of reactors. These differences are primarily associated with configuration design; however, the inclusion of AgNPs may contribute to additional inhibition effects on biological processes. Therefore, the performance strongly reflects the influence of system design and the nanoparticles interactions, suggesting that WWTP configurations with higher recirculation and reactors settings may improve their performance under variable loading conditions.

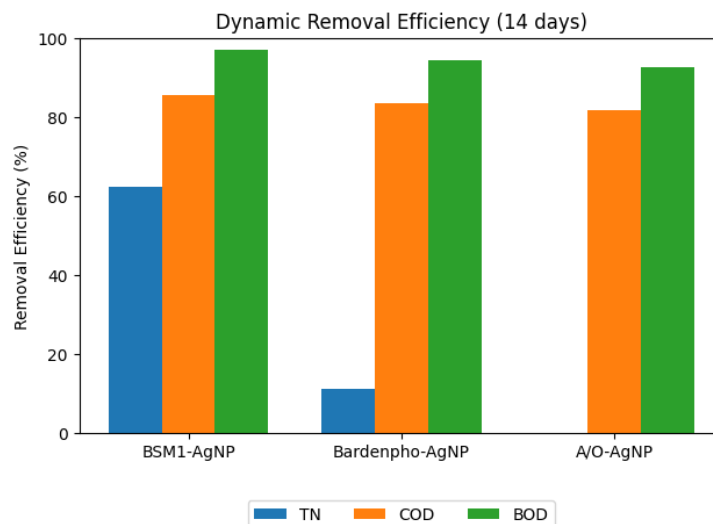


Figure 9. Removal efficiencies in dynamic state for the BSM1-AgNP, Bardenpho-AgNP, and A/O-AgNP model.

Although the model provides valuable insights into the behaviour and removal of AgNPs in different WWTPs, some degree of uncertainty remains due to assumptions in influent conditions, kinetic parameters, and the limited availability of experimental data for model calibration. Future work could include a sensitivity analysis to evaluate the influence of key operational and model parameters on system performance to improve robustness.

CONCLUSIONS

The present study was proposed as an analytical tool for evaluating different WWTPs with AgNPs, accounting for their fate mechanisms in wastewater and their possibilities of removal in wastewater treatment systems. The methodology included the design of an activated sludge model integrating the adsorption-desorption, dissolution, inhibition and chemical precipitation of AgNPs in a software; and the evaluation of the integrated systems of WWTPs. This methodology provided insight into the removal efficiency to achieve high effluent quality. The ASM had been previously calibrated and was fully developed for the software used in this study. From the analysis, the following conclusions were drawn: Modelling of the ASM-AgNP in the software's model developer appeared to be successful, showing that AgNPs can be modelled in different software considering the kinetics and stoichiometry for the biological treatment in WWTPs. AgNP removal was high across all configurations. When considering total mass removal, including both liquid and sludge, removal exceeded 98%. When considering only the liquid effluent, removal was approximately 82%. In terms of conventional treatment performance, TN removal exceeded 95% under steady state conditions, while COD and BOD removal remained above 85% and 90%, respectively. The highest effluent quality was obtained for the BSM1-AgNP model. The other two configurations showed good removal performance but presented inconsistencies with TN and CODt removal, indicating some quality limitations and the need for further optimization.

Furthermore, this area of study about emerging contaminants still needs to grow, more research needs is needed to increase awareness and improve understanding of nanoparticles. Although the present study considered three WWTP models incorporating AgNPs, there were constraints difficult to overcome because of the lack of investigation on the nanomaterial to this date. For instance, more real-world WWTPs data would help on the robustness of the models, hence more research on the industry level application should also be incentivized. Therefore, for future research the line of investigation can be carried out to include a more structured comparative analysis with AgNP dynamic data and controllers that could increase the TN removal for the two WWTP configurations that showed inconsistencies. The models proposed in the study can further

support real-world WWTPs and their operators, supporting risk evaluation and AgNPs treatment strategies, and other emerging contaminants, to finally optimize their performance. By bringing more information on the physical conditions, reactor types, nanoparticle concentration, physical properties, fate mechanisms, removal rates, and so on, the process of design and monitoring of WWTPs can be enhanced over time. Moreover, this study considers a second phase where an economic analysis will be developed to evaluate the removal efficiency versus the nanoparticles' concentrations entering WWTPs, to provide a deeper understanding of feasible solution proposals for the problem they represent to the environment and the world's population.

REFERENCES

1. V. K. Sharma, C. M. Sayes, B. Guo, S. Pillai, J. G. Parsons, C. Wang, B. Yan, and X. Ma, "Interactions between silver nanoparticles and other metal nanoparticles under environmentally relevant conditions: A review," *Sci. Total Environ.*, vol. 653, pp. 1042–1051, 2019, <https://doi.org/10.1016/j.scitotenv.2018.10.411>.
2. P. S. Bäuerlein, E. Emke, P. Tromp, J. A. M. H. Hofman, A. Carboni, F. Schooneman, P. de Voogt, and A. P. van Wezel, "Is there evidence for man-made nanoparticles in the Dutch environment?," *Sci. Total Environ.*, vol. 576, pp. 273–283, 2017, <https://doi.org/10.1016/j.scitotenv.2016.09.206>.
3. A. A. Keller and A. Lazareva, "Predicted Releases of Engineered Nanomaterials: From Global to Regional to Local," *Environ. Sci. Technol. Lett.*, vol. 1, no. 1, pp. 65–70, 2013, <https://doi.org/10.1021/ez400106t>.
4. J. Pulit-Prociak and M. Banach, "Silver nanoparticles - A material of the future...?," *Open Chem.*, vol. 14, no. 1, pp. 76–91, 2016, <https://doi.org/10.1515/chem-2016-0005>.
5. M. Noga, J. Milan, A. Frydrych, and K. Jurowski, "Toxicological Aspects, Safety Assessment, and Green Toxicology of Silver Nanoparticles (AgNPs)—Critical Review: State of the Art," *Int. J. Mol. Sci.*, vol. 24, no. 6, 2023, <https://doi.org/10.3390/ijms24065133>.
6. A. Y. R. Al-Assaf, M. A. Al-Katib, and A. Y. T. Al-Saffawi, "The Effectiveness of Bio-Silver Nanoparticles in Treating Wastewater from the Khosar River," *Egypt. J. Aquat. Biol. Fish.*, vol. 29, no. 3, pp. 555-569. ISSN 1110 – 6131.
7. R. P. Pandey, A. F. Yousef, H. Alsafar, and S. W. Hasan, "Surveillance, distribution, and treatment methods of antimicrobial resistance in water: A review," *Sci. Total Environ.*, vol. 890, no. May, p. 164360, 2023, <https://doi.org/10.1016/j.scitotenv.2023.164360>.
8. R. Sharma and A. Kumar, "Human health risk assessment and uncertainty analysis of silver nanoparticles in water," *Environ. Sci. Pollut. Res.*, vol. 31, no. 9, pp. 13739–13752, 2024, <https://doi.org/10.1007/s11356-024-32006-9>.
9. N. Rahman, M. Bharti, M. Nasir, and S. N. H. Azmi, "Performance assessment of graphene oxide decorated with silver nanoparticles as adsorbent for removal of metformin from water: Equilibrium modeling, kinetic and thermodynamic studies," *Next Mater.*, vol. 3, no. August 2023, p. 100046, 2024, <https://doi.org/10.1016/j.nxmater.2023.100046>.
10. M. Baalousha, Y. Yang, M. E. Vance, B. P. Colman, S. McNeal, J. Xu, J. Blaszcak, M. Steele, E. Bernhardt, and M. F. Hochella, "Outdoor urban nanomaterials: The emergence of a new, integrated, and critical field of study," *Sci. Total Environ.*, vol. 557–558, pp. 740–753, 2016, <https://doi.org/10.1016/j.scitotenv.2016.03.132>.
11. S. Zaheer Ud Din, K. Shah, N. Bibi, H. H. Mahboub, and M. A. Kakakhel, "Recent Insights into the Silver Nanomaterials: an Overview of Their Transformation in the Food Webs and Toxicity in the Aquatic Ecosystem," *Water, Air, Soil Pollut.*, vol. 234, no. 2, p. 114, 2023, <https://doi.org/10.1007/s11270-023-06134-w>.
12. L. Li, G. Hartmann, M. Döblinger, and M. Schuster, "Quantification of nanoscale silver

- particles removal and release from municipal wastewater treatment plants in Germany,” *Environ. Sci. Technol.*, vol. 47, no. 13, pp. 7317–7323, 2013, <https://doi.org/10.1021/es3041658>.
13. K. Ganguly, S. D. Dutta, D. K. Patel, and K. T. Lim, “Silver nanoparticles for wastewater treatment,” in *Aquananotechnology: Applications of Nanomaterials for Water Purification*, Amsterdam, Netherlands: Elsevier Inc., 2020, pp. 385–401.
 14. H. X. Shi, S. Y. Liu, J. S. Guo, F. Fang, Y. P. Chen, and P. Yan, “Potential role of AgNPs within wastewater in deteriorating sludge floc structure and settleability during activated sludge process: Filamentous bacteria and quorum sensing,” *J. Environ. Manage.*, vol. 349, no. August 2023, p. 119536, 2024, <https://doi.org/10.1016/j.jenvman.2023.119536>.
 15. A. Grosser, A. Grobelak, A. Rorat, P. Courtois, F. Vandebulcke, S. Lemièrre, R. Guyoneaud, E. Attard, and P. Celary, “Effects of silver nanoparticles on performance of anaerobic digestion of sewage sludge and associated microbial communities,” *Renew. Energy*, vol. 171, pp. 1014–1025, 2021, <https://doi.org/10.1016/j.renene.2021.02.127>.
 16. M. Henze, W. Gujer, T. Mino, and M. van Loosdrecht, “Activated Sludge Models ASM1, ASM2, ASM2d and ASM3,” Report, Lund University and IWA Taskgroup on Benchmarking of Control Strategies for WWTPs, London, UK, 2000. <https://doi.org/10.2166/9781780402369>.
 17. K. V. Gernaey, M. C. M. Van Loosdrecht, M. Henze, M. Lind, and S. B. Jørgensen, “Activated sludge wastewater treatment plant modelling and simulation: State of the art,” *Environ. Model. Softw.*, vol. 19, no. 9, pp. 763–783, 2004, <https://doi.org/10.1016/j.envsoft.2003.03.005>.
 18. J. Alex, L. Benedetti, J. Copp, K. V. Gernaey, U. Jeppsson, I. Nopens, M. Pons, L. Rieger, C. Rosen, J. P. Steyer, P. Vanrolleghem, and S. Winkler, “Benchmark Simulation Model No. 1 (BSM1),” Report, LUTEDX/(TEIE-7229)/1-62, Lund University and IWA Taskgroup on Benchmarking of Control Strategies for WWTPs, Lund, Sweden, 2008.
 19. X. Wu, Y. Yang, G. Wu, J. Mao, and T. Zhou, “Simulation and optimization of a coking wastewater biological treatment process by activated sludge models (ASM),” *J. Environ. Manage.*, vol. 165, pp. 235–242, 2016, <https://doi.org/10.1016/j.jenvman.2015.09.041>.
 20. Y. Tian, Z. Hu, H. Cheng, J. Xiao, and L. Wu, “Process Modeling and Its Application in Municipal Wastewater Treatment Plant Based on Seasonal Temperature Variations: A Case Study in Eastern China,” *Water (Switzerland)*, vol. 17, no. 7, pp. 1–18, 2025, <https://doi.org/10.3390/w17070994>.
 21. Y. Zhu, H. Zhang, H. Sun, Y. Zhang, L. Yang, C. Liu, X. Yang, and Y. Liu, “Effect of silver nanoparticles on biological nitrogen removal in sequential batch wastewater treatment process: Microbial communities, functional genes, and interactions,” *J. Water Process Eng.*, vol. 70, no. January, 2025, <https://doi.org/10.1016/j.jwpe.2025.107114>.
 22. Z. Fan, Y. Huang, Y. Duan, Z. Tang, and X. Yang, “Effects of silver nanoparticles and various forms of silver on nitrogen removal by the denitrifier *Pseudomonas stutzeri* and their toxicity mechanisms,” *Ecotoxicol. Environ. Saf.*, vol. 269, no. August 2023, p. 115785, 2024, <https://doi.org/10.1016/j.ecoenv.2023.115785>.
 23. Y. Guo, N. Cichocki, F. Schattner, R. Geffers, H. Harms, and S. Müller, “AgNPs change microbial community structures of wastewater,” *Front. Microbiol.*, vol. 10, no. JAN, pp. 1–12, 2019, <https://doi.org/10.3389/fmicb.2018.03211>.
 24. L. Chen, W. Feng, J. Fan, K. Zhang, and Z. Gu, “Removal of silver nanoparticles in aqueous solution by activated sludge: Mechanism and characteristics,” *Sci. Total Environ.*, vol. 711, p. 135155, 2020, <https://doi.org/10.1016/j.scitotenv.2019.135155>.
 25. H. Yu, H. Zhang, C. Zhang, R. Wang, S. Liu, R. Du, and W. Sun, “Advances in treatment technologies for silver-containing wastewater,” *Chem. Eng. J.*, vol. 496, no. July, p. 153689, 2024, <https://doi.org/10.1016/j.cej.2024.153689>.

26. P. Vilela, H. Liu, S. C. Lee, S. Hwangbo, K. J. Nam, and C. K. Yoo, "A systematic approach of removal mechanisms, control and optimization of silver nanoparticle in wastewater treatment plants," *Sci. Total Environ.*, vol. 633, pp. 989–998, 2018, <https://doi.org/10.1016/j.scitotenv.2018.03.247>.
27. F. Fu and Q. Wang, "Removal of heavy metal ions from wastewaters: A review," *J. Environ. Manage.*, vol. 92, no. 3, pp. 407–418, 2011, <https://doi.org/10.1016/j.jenvman.2010.11.011>.
28. P. Cervantes-Avilés, Y. Huang, and A. A. Keller, "Incidence and persistence of silver nanoparticles throughout the wastewater treatment process," *Water Res.*, vol. 156, pp. 188–198, 2019, <https://doi.org/10.1016/j.watres.2019.03.031>.
29. Hydromantis, "GPS-X Technical Reference," Report, Hydromantis, Hamilton, Canada, 2017.
30. Hydromantis, "GPS-X Model Developer Guide," Report, Hydromantis, Hamilton, Canada, 2019.
31. M. S. Kadri, R. R. Singhanian, D. Haldar, A. K. Patel, S. K. Bhatia, G. Saratale, B. Parameswaran, and J. S. Chang, "Advances in Algomics technology: Application in wastewater treatment and biofuel production," *Bioresour. Technol.*, vol. 387, no. July, p. 129636, 2023, <https://doi.org/10.1016/j.biortech.2023.129636>.

UNCORRECTED PROOF